

# Bringing Solar Site Analysis to Smartphones

Joseph Ranalli  
Matthew Caccese  
Penn State Hazleton  
76 University Dr.  
Hazleton, PA 18202  
jranalli@psu.edu  
mxc5371@psu.edu

Jesse Fox  
Innovatrix Labs, Inc.  
103 Rotary Drive, Suite #2  
West Hazleton, PA 18202  
jfox@innovatrixlabs.com

## ABSTRACT

Performing a site analysis is an important first step in planning a solar installation. This paper details progress made in development and validation of an Android smartphone-based application to assist in the site analysis process. The methodology used is based on techniques from literature and standard practice. Hourly typical meteorological year (TMY3) solar resource data is used to estimate the energy available to a potential solar collector. These estimates are extended to represent plane-of-array irradiation using a standard diffuse-sky model. The user is prompted to trace the horizon using the phone's camera in order to determine the presence of objects that may introduce shading. This shading data can be used to calculate the impact on the estimated resource, or can be used to generate solar access inputs to other standard software. Techniques found in literature were used to compute optimum collector orientations based on the shaded solar access. The calculations within the app were compared with those made using the NREL System Advisor Model software. Data from the app can be stored for subsequent transfer to a computer for further processing or integration with other software tools. Some limitations associated with using the smartphone platform for this purpose will be discussed. The chief advantages offered by this software are its ability to make use of existing smartphone hardware and documentation of the methodology in non-proprietary venues.

## 1. INTRODUCTION

One important part of planning a solar installation is performing a site analysis. This process involves an assessment of the solar resource, providing an estimate of the potential output. Such estimates can be used to plan a solar installation or to evaluate the output of an existing

array. Typical data needed to conduct a solar site survey include the predominant weather patterns in the location as well as the proposed site's solar access. Solar access refers to identification of obstacles that may cast shade onto the collector, restricting the ability to collect solar energy at certain times of day. Shading is of particular concern to photovoltaic installations, but impacts solar thermal systems as well.

A variety of methods and tools already exist to perform the shading portion of a solar site analysis. These may be as simple as using a plumb and protractor to sight obstacles and plot them on a sun chart. Commercial tools are also available in the form of electronic hardware that can identify obstacles automatically through digital image processing. Digital tools typically allow resource analysis as well using user-specified weather files as inputs. This paper discusses ongoing work aimed at providing a simple, free, well-documented site-analysis tool that works on a common hardware platform, namely an Android smartphone.

## 2. DOCUMENTATION OF METHODOLOGY

Many commercial tools already exist for performing solar site analysis. Duluk *et al.* [1] compared the features and performance of several of these tools and conclude that there are still some shortcomings in the site analysis tool marketplace. None of the tools they tested were able to adequately account for differences between direct, diffuse and ground reflected irradiance on a surface in the resource determination. Additionally, they note that comparisons between the tools do not produce consistent results, casting questions on the accuracy of these approaches.

The software developed in this study aims to provide a complete description of its methodology in the academic literature to allow investigation regarding any questions as

to accuracy or effectiveness of the approach. In addition, this software is open-source and can be contributed to or modified by anyone with the ambition to improve upon its functionality. The software was created to operate on Android smartphones, and as such the majority of the code uses the Java programming language. The Android deployment platform was chosen in order to take advantage of the existing technological and sensor capabilities present in smartphones, which have become nearly ubiquitous. The primary goal of the software is to provide estimates of the available solar irradiance in a given location and to allow measurement of the local horizon and its impact on this irradiance. Several features of the hardware are utilized to create these estimates.

### 2.1. Solar Resource Data

Solar resource data about a given location is obtained in typical meteorological year format, TMY3 [2]. These data sets are produced by the National Renewable Energy Lab (NREL) using data from the National Solar Radiation Database (NSRDB) [3] and represent a “typical” year in a given location. Depending on the location used, TMY3 files include irradiance data collected over 30 years (1976-2005) or 15 years (1991-2005). Since TMY3 data are chosen to represent a typical year, the TMY3 data sets lack extreme values and cannot be used to represent best-case or worst-case scenarios. Rather, they should only be used to estimate long-term overall performance, as opposed to models of actual day-to-day variation [2].

TMY3 data files contain a great deal of location-specific, hourly weather data representing a typical year. The fields used by the software are: Global Horizontal Irradiance ( $G_{g,h}$ ), Direct Normal Irradiance ( $G_{b,n}$ ) and Diffuse Horizontal Irradiance ( $G_{d,h}$ ). Only two of these irradiance values are used at any given time, as the third can be calculated from the others. At the present time, we do not incorporate the available uncertainty values for these measurements, nor do we make use of any actual photovoltaic cell modelling (e.g. efficiency or temperature effects) to produce a power output estimate. Rather the estimates of solar availability used in the software are currently based on plane-of-array irradiance only, and represent the solar input to a collection system.

The geographically closest TMY3 data file is automatically chosen by the software based on either phone-reported location or user latitude/longitude input. Alternatively, users can override the closest file to specify a TMY3 data file of their own choosing. As local storage of the data files would be prohibitive, the data are read directly from the NSRDB servers, requiring an active internet connection for solar resource estimates to be performed.

### 2.2. Computing Plane-Of-Array Irradiance

In order to estimate the solar resource available to a solar collector, we consider a plane array oriented at a given tilt ( $\beta$ ) and azimuth ( $\gamma_c$ ). We determine the tilted (plane-of-array) global irradiance ( $G_{g,t}$ ) estimates using the modelling methodology of Muneer [4], following the implementation by Lave and Kleissl [5]. Lave and Kleissl previously applied this methodology using modelled NSRDB data to estimate optimum tilt-azimuth orientations throughout the continental US. Other irradiance model options (notably Perez *et al.* [6]) can be found in the literature and may be incorporated into the software in the future.

As part of the  $G_{g,t}$  calculation, the hourly solar geometry in terms of the hourly altitude and azimuth ( $\alpha_s$  and  $\gamma_s$ , respectively), must be calculated. Methodologies for obtaining these solar angles are available in a variety of sources, an example being the text by Kalogirou [7]. The TMY3 weather files present data for the period ending at the hour shown (listed in Local Standard Time). We assume that the average position of the sun over the course of the hour occurs half way through this period [5]. Therefore, corrections are applied to convert Local Standard Time (LST) to Solar Time, and solar altitude and azimuth are calculated for the preceding mid-hour point (i.e. 30 minutes before the time shown in the file). So the data point in the file indicated at a time stamp of 09:00 LST is computed at an effective time of 08:30 LST, which is then converted to solar time based on the longitude and the equation of time in order to compute the solar position.

The Muneer methodology requires inputs of two of the three irradiances, along with the latitude/longitude of the location and the array orientation. In order to evaluate the relationship, the beam component of the irradiance must be corrected to horizontal ( $G_{b,h}$ ) to account for the incidence angle, as follows:

$$G_{b,h} = G_{b,n} * \sin \alpha_s$$

Then, the three components are related by:

$$G_{g,h} = G_{d,h} + G_{b,h}$$

The software defaults to using the  $G_{b,n}$  and  $G_{d,h}$  as inputs and obtaining the  $G_{g,h}$  via calculation. This differs from Muneer [4] and Lave and Kleissl [5], who use global and diffuse horizontal terms as the basis for calculation. Our reason for diverging from the references is to match the default behavior of the NREL System Advisor Model (SAM), which also defaults to utilizing  $G_{b,n}$  and  $G_{d,h}$  to calculate  $G_{g,h}$  [8].

The plane-of-array (tilted surface) global irradiance ( $G_{g,t}$ ) is computed as the sum of three components. Each is

measured on the tilted surface. They are: the Direct Beam ( $G_{b,t}$ ), the Sky Diffuse ( $G_{d,t}$ ) and the Ground Reflected ( $G_{r,t}$ ). Each component is constrained to zero should the computation produce a negative (i.e. non-physical) result.

The direct beam irradiance on the tilted surface,  $G_{b,t}$  is computed using  $\theta_i$ , the incidence angle between the sun and the array normal:

$$G_{b,t} = G_{b,h} \frac{\cos \theta_i}{\sin \alpha_s}$$

Further,  $G_{b,t}$  is assumed to be exactly zero at all times when the sun is below the horizon ( $\alpha_s < 0^\circ$ ) and when the incidence angle indicates that the sun is behind the collector ( $\theta_i > 90^\circ$ ).

The sky diffuse irradiance is a multi-step calculation. First a clearness index,  $K_b$ , based on the beam irradiance, is computed:

$$K_b = \frac{G_{b,h}}{\epsilon G_{sc,n} \sin \alpha_s}$$

In this equation,  $G_{sc,n}$  is the solar constant whose value is  $G_{sc,n} = 1361 \text{ W/m}^2$ . The term  $\epsilon$  is the correction for the eccentricity of the earth's orbit according to the formula [4]:

$$\epsilon = 1 + 0.033 \cos \left( 360^\circ \frac{n-2}{365} \right)$$

where  $n$  represents the integer day of the year. The clearness index and panel tilt are used to compute the value of an empirical function,  $f$ , that will be used in the correlation for diffuse irradiance. Following the methodology of Lave and Kleissl [5], we adopt a correlation proposed for Southern Europe as representative of the United States.

$$f = \cos^2 \left( \frac{\beta}{2} \right) + (0.00263 - 0.7120 K_b - 0.6883 K_b^2) * \left[ \sin \beta - \beta \cos \beta - \pi \sin^2 \left( \frac{\beta}{2} \right) \right]$$

Care must be taken that regardless of whether degree or radian angles are used throughout, the term  $\beta \cos \beta$  requires that the value of  $\beta$  be measured in radians for the scalar multiple. Finally, a value of the diffuse irradiance on the tilted surface can be computed as:

$$\frac{G_{d,t}}{G_{d,h}} = f * (1 - K_b) + K_b \frac{\cos \theta_i}{\sin \alpha_s}$$

This value is considered to be valid for all solar altitudes above  $5.7^\circ$ . For solar altitudes below  $5.7^\circ$ , a modified form is used as described by Page [9]:

$$\frac{G_{d,t}}{G_{d,h}} = \cos^2 \left( \frac{\beta}{2} \right) * \left[ 1 + K_b * \sin^3 \left( \frac{\beta}{2} \right) \right] * [1 + K_b * \cos^2 \theta_i * \sin^3(90 - \alpha_s)]$$

The ground reflected term,  $G_{r,t}$  is computed as:

$$G_{r,t} = \frac{1 - \cos \beta}{2} \rho_g G_{g,h}$$

The software assumes a constant value for the ground albedo,  $\rho_g = 0.2$ . This choice is made even in the presence of albedo data in the TMY3 file. The reasoning for this choice is that albedo data is only rarely present in the TMY3 files, and incorporating these values could cause month-to-month "artificial" variability when present. Ground reflected irradiance is generally one or two orders of magnitude smaller than the other terms, so in any case, this does not significantly impact the overall solar resource estimates.

These three plane-of-array values are combined to compute the global irradiance on the tilted surface:

$$G_{g,t} = G_{b,t} + G_{d,t} + G_{r,t}$$

This value is considered to be the "solar resource" available to a potential collector.

### 2.3. Shading Methodology

Shading is determined on a binary basis using a horizon profile (discussed in Section 2.5). Every hourly solar altitude is compared to the horizon profile. If the solar altitude falls below the horizon it is considered to be shaded and the previously computed irradiance is modified appropriately. At present we do not consider the possibility of interpolating to estimate part-hour shading, and look instead only at point results based on the hourly sun positions.

Testing to determine whether the point falls below the horizon is performed by using a modification of common point-in-polygon algorithms. In this case, the polygon formed by the horizon is assumed to encircle the point straight down from the user ( $-90^\circ$  in altitude). Testing on a solar position location is then performed by counting intersections between the horizon and a line connecting the point at an altitude of  $-90^\circ$  and the point of interest. An even number of intersections indicates shading, while an odd number indicates that the point is above the horizon. This approach allows the horizon to be multi-valued in azimuth, an event that might be expected if considering obstruction by a lone tree with a slender trunk but large canopy.

While several shading approaches are available in literature, Drif *et al.* [10] recommend a method that accounts separately for the anisotropic (circumsolar, isotropic and

horizon) diffuse terms present in the total diffuse irradiance used by the Muneer and Perez models. Specifically, the circumsolar diffuse irradiance is assumed to be forced to zero by shading, while the other terms are unchanged. At present the approach adopted by this study is a simpler one, though future work aims to include an option to perform this additional analysis.

Presently, all hours determined to have shading obstructions are modified such that the beam component of the irradiance ( $G_{b,t}$ ) is assumed to be zero. The diffuse and ground reflected terms are not adjusted. This behavior is similar to that of SAM [8]. SAM assumes that on an hourly basis, only the beam irradiance is affected by a shading factor, while sky diffuse irradiance may be reduced by a single scaling factor affecting all hours of the year. At present, the software developed in this project does not consider scaling for the diffuse term; however, the horizon data obtained could be used to calculate such a view factor correction in the future.

#### 2.4. Device Location and Orientation

The location of the phone is used in two ways. The first use is to identify the geographically nearest TMY3 station, which does not require a great deal of accuracy due to the spacing of the stations. The second use of the location is to provide an origin for performing the sun position calculations. The software uses the phone's location obtained via GPS, Wi-fi or Cell Towers depending on user preferences. The accuracy of the location depends on the specific hardware used, but the hardware reported accuracy had a worst case error of approximately 1.5 km for the Cell Towers, with Wi-fi and GPS on the order of 10 m. An error in surface position measurement of 1.5 km results in a latitude error of less than  $0.05^\circ$ . Position errors have a linear influence on the sun's altitude at solar noon. Thus, this worst case location uncertainty of  $0.05^\circ$  in the sun altitude was considered negligible and any of the location providers available were considered sufficient.

The device orientation is measured using the Android platform's built-in *Rotation Vector* sensor. This composite sensor combines gyroscopic, magnetic and accelerometer readings to produce a single reading of the absolute angular orientation of the device. This approach enables the software to make use of additional sensor data provided by the operating system when that data is available on the hardware itself, and provides some measure of platform independence. The default axes are transformed to reflect the altitude and azimuth coordinates commonly used in solar power calculations. The roll of the camera is only used in appropriately transforming the on-screen display. Future investigation is needed to evaluate the accuracy of these position sensors and their impact on the horizon measurement.

#### 2.5. Horizon Measurement

The horizon is obtained by geometric tracing. The smartphone device screen is used to display the field of view as seen by the rear-facing camera. The user is prompted to angle the device to trace out the upper boundary of the shading obstacles using a cross marker in the center overlaid in the camera field of view. During this process the azimuth and altitude of the smartphone are recorded continuously, producing a list of shading altitudes at each azimuth the phone is aimed at.

Under the point-in-polygon shading test methodology, the horizon profile must be represented by a closed curve. This is accomplished by connecting the first and last points of the tracing. While this enables the user to begin and end at an arbitrary azimuth, it does require that more than  $180^\circ$  of azimuth are spanned by the tracing to produce an accurate result. Future work aims to improve the reliability of the horizon profile acquisition process to increase its user-friendliness, including possible implementation of image processing to acquire horizons directly from photos.

#### 2.6. Optimization

Following the approach of Lave and Kleissl [5], the software implements a nonlinear function optimization to compute the collector orientation (tilt,  $\beta$  and azimuth,  $\gamma_c$ ) that would produce the highest plane-of-array irradiance for the weather file selected. This approach is extended to include the impacts of the shading analysis. Shaded optimization is performed on a set of weather data with the shading conditions applied (beam irradiance set to zero when shaded). The results of this calculation are consistent with expectations, e.g. shading in the afternoon results in an eastward shift in the optimum orientation.

#### 2.7. Software outputs

The software on the smartphone produces comma separated value (CSV) files that can be conveniently read by a computer. The base project file contains some reference information about the current "project" file. This includes the base latitude and longitude, the name of the TMY3 file being used, the tilt and azimuth specified for a collector and the optimum tilt and azimuth for a collector in that location. Additional CSV files are created that contain a subset of the weather data used, and the hourly plane-of-array irradiances. A separate file is generated including the horizon data as a list of azimuth, altitude ordered pairs (if such a horizon measurement was performed by the user).

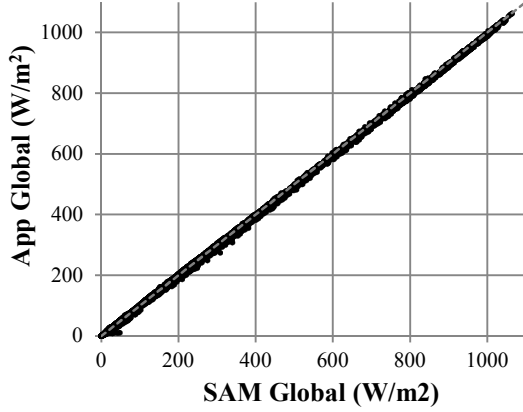


Fig. 1: Plane-of-array global irradiance comparison for Wilkes-Barre/Scranton. Line represents perfect match.

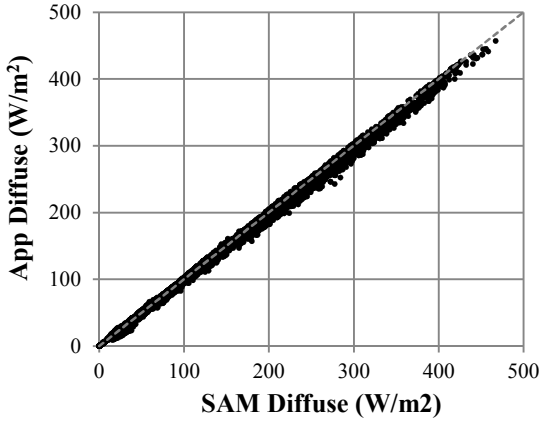


Fig. 2: Plane-of-array diffuse irradiance comparison for Wilkes-Barre/Scranton. Line represents perfect match.

Pictures can be acquired including an overlay of the sun's path on different days throughout the year. Files are produced along with the images that contain the phone orientation that corresponds to each frame. Further work is needed to embed image processing to identify the horizon directly from the images and/or to produce spherical panoramic images similar to those produced by other commercial site survey tools.

### 3. VALIDATION

The computations performed by the software were validated against calculations performed using the SAM Application Program Interface (API). The SAM API allows easy determination of the plane-of-array irradiance that would be used as an input in subsequent SAM system analyses. Though SAM uses the Perez model, rather than the Muneer

model employed here, results were found to be in close agreement. Fig. 1: Plane-of-array global irradiance comparison for Wilkes-Barre/Scranton. Line represents perfect match. Fig. 1 and Fig. 2 compare outputs from the software developed in this study and the SAM API for a collector with a tilt of  $\beta = 20^\circ$  and an orientation pointed toward the equator ( $\gamma_c = 0^\circ$ ). Perfect agreement would be indicated by a line passing through the origin with a slope of unity.

The results shown all utilize data from the nearest TMY3 site to the authors: Wilkes-Barre Scranton International Airport. Similar results are obtained for other weather files tested. Some discrepancies were observed in the ground reflected results (not shown). This error resulted from the fact that SAM makes use of the albedo data present in TMY3 files when available, while our method used a fixed albedo of  $\rho_g = 0.2$ , as previously discussed. As stated, ground reflected irradiance typically accounts for less than 1% of the total irradiance, so this difference does not significantly influence the plane-of-array total results that are displayed in Fig. 1.

As an accompaniment to the visual representations in the figures, statistical error analysis of the data can be found in Table 1. We analyze the percent error ( $e$ ) using two different statistical measures: root mean square error (RMSE) and mean bias error (MBE), assuming the SAM data is the true value. Data points with an irradiance calculated by SAM of exactly zero are discarded to prevent their influence on the statistics.

The measures are defined as follows:

$$e = G_{x,t}|_{APP} - G_{x,t}|_{SAM}$$

$$RMSE = \sqrt{\frac{1}{n} \sum_{i=1}^n (e^2)}$$

$$MBE = \frac{1}{n} \sum_{i=1}^n (e)$$

All results in Table 1 are for Wilkes-Barre/Scranton International Airport, though other locations were observed to have similar results. All data are computed at an azimuth of  $0^\circ$  (due south). Variation with azimuthal change is observed to be small compared to tilt (increase of  $3 \text{ W/m}^2$  in RSME over  $30^\circ$  azimuthal shift). It is evident that the error increases with increasing tilt. However, when considering the magnitude of the RSME as compared to the overall magnitude of the irradiance, it remains relatively small, even in the limiting case. The highest error observed for the locations and orientations tested was an RSME value of

32.0 W (Orlando, FL, tilt of 90° with an azimuth of 0°). Normalized by the peak irradiance, this is a discrepancy of approximately 3%. Typical uncertainties of the irradiance values in the source TMY3 files are around 10%, so the errors in the comparison with SAM are well within reason.

TABLE 1: STATISTICAL ERROR FOR IRRADIANCE

Tilt	$G_{g,t}$		$G_{d,t}$	
	RMSE (W/m <sup>2</sup> )	MBE (W/m <sup>2</sup> )	RMSE (W/m <sup>2</sup> )	MBE (W/m <sup>2</sup> )
20°	6.6	-3.6	6.5	-3.5
40°	9.8	-4.3	9.5	-4.3
60°	11.5	-3.0	10.9	-3.1
80°	13.1	-0.9	12.1	-1.2
90°	14.0	0.2	12.8	-0.2

One other factor observed is that the Muneer methodology we employ tends to under-predict the POA irradiance as compared to the Perez methodology employed by SAM. This is clearly visible in Fig. 1 and Fig. 2, and numerically indicated by the MBE. The error in general is dominated by the error in the diffuse irradiance, with beam irradiance error typically less than half the diffuse error. The higher level of agreement seen in the beam irradiance is expected due to the fact that the beam component results from a simpler calculation that is common to both models; it depends only on the known  $G_{b,h}$  and the solar geometry relative to the collector.

Table 2 contains comparisons between the optimum collector tilt and azimuth, along with the corresponding annual irradiation at the optimum orientations. The comparison is between results computed by our implementation of the methods and computations made using the SAM API. The test locations are chosen to match those of Lave and Kleissl. Interestingly, while the results between the app and SAM are in close agreement, they diverge from Lave and Kleissl’s results, which we attribute to our use of TMY3 compared to their use of 10-years of SUNY-modelled data. The maximum angular discrepancy in any direction between our computations and those based on SAM is 1.3° (Orlando, FL, tilt values). The maximum discrepancy in annual irradiation at the optimum orientation is 0.03 GWh/yr, which corresponds to an error of around 1.5%.

Comparisons of the shading algorithm were unavailable due to the difficulty in extracting shaded irradiance values from SAM computations. Given that the shading algorithm is relatively simple (blocking beam irradiance only), we consider the comparisons of the plane-of-array irradiance sufficient to establish preliminary confidence in the shading methodology.

TABLE 2: OPTIMUM ORIENTATION COMPARISON

Station (Long, Lat)	App (deg)		SAM (deg)	
	Tilt	Azi.	Tilt	Azi
Orlando, FL (81.3 W, 28.4 N)	27.1	11.3 E	25.8	10.7 E
	1.78 MWh/m <sup>2</sup> yr		1.79 MWh/m <sup>2</sup> yr	
Dallas, TX (97.0 W, 32.9 N)	29.3	7.5 W	29.4	7.5 W
	1.96 MWh/m <sup>2</sup> yr		1.99 MWh/m <sup>2</sup> yr	
Phoenix, AZ (112.0 W, 33.4 N)	32.0	2.0 E	31.7	2.3 E
	2.37 MWh/m <sup>2</sup> yr		2.39 MWh/m <sup>2</sup> yr	
Los Angeles, CA (118.4 W, 33.9 N)	31.4	10.5 W	31.0	10.2 W
	2.05 MWh/m <sup>2</sup> yr		2.06 MWh/m <sup>2</sup> yr	
St. Louis, MO (90.4 W, 38.8 N)	33.4	1.9 E	33.4	1.6 E
	1.74 MWh/m <sup>2</sup> yr		1.76 MWh/m <sup>2</sup> yr	

#### 4. DISCUSSION AND CONCLUSIONS

The software developed allows an Android smartphone to function as a solar site survey tool. Validation shows that the results produced are in close agreement with those obtained from standardized software tools used in the field albeit with use of a different irradiance model. Some need for further validation exists, particularly as it relates to the bias observed in the modeled data. We plan to determine whether this is an artifact of the difference in modelling methodology, or whether some other discrepancy in the calculation exists. Regardless, the data currently show agreement that falls within the baseline uncertainty in the source data.

This software offers several advantages. It allows users to take advantage of the capabilities of existing hardware; smartphones are prevalent and already possess the functionality necessary to this type analysis on a mobile platform. It also offers these functions using an open source code base that can be investigated and modified by users. Lastly, the methodology is being disclosed in literature, ensuring that it is subject to peer review and improvement as part of the academic process. Though development is ongoing, this tool can already provide easy access to baseline site survey analysis.

Several areas have been identified for future improvement. User-friendliness is a major concern given the smartphone platform being employed. We plan to address this area in part as we receive feedback from users. We will also track feedback to determine whether the outputs being provided are sufficient or whether additional data might be needed.

Testing is also ongoing as to the sensitivity of the methodologies to variations in input parameters, to provide a better idea of the uncertainties associated with the smartphone platform as compared to other tools.

The flexibility of the methodology will be improved upon by adding the option for other irradiance modelling approaches (e.g. Perez), and by improving upon the method by which shading impacts are addressed. Future plans also include integration of image processing capabilities to identify the horizon directly from images, rather than relying on the horizon tracing interface. Continued testing and comparison against standard tools will be performed as these improvements are made to ensure that this software produces results that can be used with the same confidence of established methods.

In closing, we would like to identify this work as in-progress and would gladly invite bug reports, comments and suggestions or direct contributions to the code from the community at large.

## 5. ACKNOWLEDGEMENTS

The authors wish to acknowledge the contributions of Kurt Schaarschmidt and Niraj Patel in creating the software.

## 6. REFERENCES

- [1] Duluk, S., Nelson, H. and Kwok, A., Comparison Of Solar Evaluation Tools: From Learning To Practice, Proceedings of the 42<sup>nd</sup> ASES Annual Conference, American Solar Energy Society, 2013
- [2] Wilcox, S. and Marion, W., Users Manual for TMY3 Data Sets, NREL/TP-581-43156, National Renewable Energy Laboratory, 2008
- [3] Wilcox, S., National Solar Radiation Database 1991-2010 Update: User's Manual, NREL/TP-5500-54824, National Renewable Energy Laboratory, 2012
- [4] Muneer, T., Solar Radiation and Daylight Models, Elsevier, 2004
- [5] Lave, M. and Kleissl, J., Optimum fixed orientations and benefits of tracking for capturing solar radiation in the continental United States, Renewable Energy, Vol 34, 2011
- [6] Perez, R., Ineichen, P., Seals, R., Michalsky, J. and Stewart, R., Modeling Daylight Availability and Irradiance Components from Direct and Global Irradiance, Solar Energy, Vol 44, No 5, 1990
- [7] Kalogirou, S., Solar Energy Engineering, Academic Press, 2009
- [8] National Renewable Energy Lab, System Advisor Model Version 2014.1.14 (SAM 2014.1.14), National Renewable Energy Laboratory, 2014
- [9] Page, J., The Role of Solar Radiation Climatology in the Design of Photovoltaic Systems, Practical Handbook of Photovoltaics, Elsevier, 2003

[10] Drif, M., Perez, P.J., Aguilera, J. and Aguilar, J.D., A new estimation method of irradiance on a partially shaded PV generator in grid-connected photovoltaic systems, Renewable Energy, Vol 33, 2008